Conf-911111--26

PNL-SA--19959

DE92 006484

IRRADIATION CREEP AND CREEP RUPTURE OF TITANIUM-MODIFIED AUSTENITIC STAINLESS STEELS AND THEIR DEPENDENCE ON COLD WORK LEVEL

F. A. Garner
C. R. Eiholzer
A. S. Kumar
M. L. Hamilton
M. B. Toloczko

November 1991

Presented at the
5th International Conference on
Fusion Reactor Materials
November 17-22, 1991
Clearwater, Florida

Work supported by
the U.S. Department of Energy
under Contract DE-AC06-76RLO 1830

Pacific Northwest Laboratory
Richland, Washington 99352

IRRADIATION CREEP AND CREEP RUPTURE OF TITANIUM-MODIFIED AUSTENITIC STAINLESS STEELS AND THEIR DEPENDENCE ON COLD WORK LEVEL

- F. A. Garner and M. L. Hamilton Pacific Northwest Laboratory, C. R. Eiholzer Westinghouse Hanford Company , M. B. Toloczko University of California at Berkeley and A. S. Kumar University of Missouri-Rolla.

OBJECTIVE

The objective of this effort is to provide insight into the factors that control the creep response of structural steels during neutron irradiation.

SUMMARY

A titanium-modified austenitic type stainless steel was tested at three cold work levels to determine its creep and creep rupture properties under both thermal aging and neutron irradiation conditions. Both the thermal and irradiation creep behavior exhibit a complex non-monotonic relationship with cold work level that reflects the competition between a number of stress-sensitive and temperature-dependent microstructural processes. Increasing the degree of cold work to 30% from the conventional 20% level was detrimental to its performance, especially for applications above 550°C. The 20% cold work level is preferable to the 10% level, in terms of both in-reactor creep rupture response and initial strength.

PROGRESS AND STATUS

Introduction

The development of austenitic steels for fusion or breeder reactor service requires choosing not only the optimum composition but also the optimum processing history. Stainless steels are usually specified to be in the cold worked condition, both to provide sufficient strength and to resist void swelling. Cold working to progressively higher levels is known to lead to a continuous but diminishing reduction in swelling.[1] Since the irradiation creep rate is known to be proportional to the concurrent swelling rate,[2] it appears reasonable to assume that the creep rate should also be reduced at higher cold work levels. In fact, however, other factors come into play when irradiation and stress act on the steel simultaneously at elevated temperatures. Thus, the creep rate and creep rupture life may not be monotonic functions of the cold work level. The objective of this study is to provide some insight into the relationship between cold work and creep for the titanium-modified austenitic alloys employed in the U.S. fusion and breeder reactor materials programs.

Experimental Procedure

The interplay between the various factors that influence the response of the cold worked alloy was investigated in a series of thermal and irradiation experiments involving either creep or creep rupture behavior. Thin walled gas-pressurized tubes 2.24 cm long with outer and inner diameters of 4.57 and 4.17 mm, respectively, were used. The tubes were constructed from a titanium-modified steel (D9 production heat 83508) and prepared in each of the 10%, 20% and 30% cold work levels. Larger tubes with outer and inner diameters of 5.84 and 5.08 mm and 2.82 cm long were also prepared at the 20% cold work level.

Two types of thermal control tests were performed. In the first type of test, end caps of 316 stainless steel were gas-tungsten-arc welded to one end of each tube and a gas inlet tube was welded to the other end. This configuration was used to conduct stress rupture tests at constant pressure in static argon gas at temperatures ranging from 538 to 760°C and hoop stresses ranging from 20 to 400 MPa. Failure of these constant pressure tests was detected by a sudden rise of retort pressure. Strains were measured only after specimen failure.

In the second type of thermal control test, both ends of the tubes were fitted with D9 end caps by electron beam welding and the tube was then pressurized with helium gas, after which the inlet hole in the top end cap was sealed with a laser beam. These tubes were heated at temperatures ranging from 550 to 750°C for times as long as 8,000 hours. The tubes were removed periodically and their diameters measured using a non-contacting laser system.[(3)] This type of test approximates a constant stress in the tube wall. As the tube expands in diameter, the effect of wall thinning on increasing the hoop stress balances out the decrease due to the drop in gas pressure. This is in contrast to the situation in the constant pressure tubes used in the stress rupture experiments, where the stress level in the tube wall rises slightly as the tube expands.

In-reactor tests using the sealed pressurized tube specimens were also conducted at temperatures between 400 and 667°C. Some of the tubes irradiated at temperatures of 575°C and above contained a unique isotopic mixture of krypton and xenon tag gases added to the helium fill gas. These tag gas mixtures were included only in tubes at the 10% and 20% cold work levels. At the 20% level only the larger tube size contained the tag gas, even though both size tubes were irradiated in the experiment.

After sealing the tubes, the preirradiation diameter were measured at room temperature and the specimens were loaded into the Materials Open Test Assembly (MOTA), which was then placed into the Fast Flux Test Facility (FFTF). The specimens were actively maintained within ±5°C of their target temperature during irradiation.

When a gas tagged tube failed during a reactor cycle, the event was detected by spectrographic analysis of reactor cover gas samples and the failure time was recorded.[4] All tubes were removed from MOTA at the end of each irradiation sequence and their diameters were measured regardless of whether they had failed or not. Tubes that had not failed were returned for the next irradiation sequence.

As will be discussed in the next section, the 30% cold worked tubes in the first several irradiation sequences were found to exhibit much larger strains at the higher irradiation temperatures, and also to develop larger levels of instability in thermal aging studies. In addition, an expanded emphasis on ferritic steels required a reduction in MOTA volume reserved for austenitic alloys. A decision was, therefore, made to remove the 30% cold worked tubes from MOTA at the end of the second irradiation cycle. The 10% and 20% cold worked tubes were returned for a third cycle and reached a peak neutron fluence of 1.7×10^{22} n/cm^2 (E > 0.1 MeV).

Hardness measurements were performed on cross sections of the tubing in the as-received state and also on thermally aged specimens (650, 704, 760°C) for times as long as 3,000 hours.

Results: Stress Rupture

Figure 1a summarizes the overall behavior of the stress rupture data for 10% and 20% cold worked tubes, both of which were 4.57 mm in outer diameter. The actual data are plotted in Figures 1b and 1c as a function of the Larson Miller Parameter (LMP) to facilitate comparisons between the thermal and the in-reactor rupture data, which were derived in slightly different but overlapping temperature ranges.

The LMP is determined here as $T[13.5 + \log(t_r)]$, where T is the temperature in Kelvin and t_r is the time to rupture in hours. Note that the 10% cold worked condition exhibits slightly better thermal stress rupture behavior than the 20% cold work condition. The difference in the slope of the lines describing the 10 and 20% conditions suggests that the latter recovers more quickly than the former, a conclusion that is consistent with the results of earlier studies on AISI 304 and 316 stainless steel.(5)

Also shown in Figures 1b and 1c are comparisons between the thermal control and in-reactor data.(6) The in-reactor stress rupture lifetimes are significantly shorter than the corresponding thermal control data for rupture times greater than ~2,000 hours, although as reported earlier,(3) the rupture times are comparable below ~2,000 hours. For irradiation temperatures greater than 605°C, the limited in-reactor data suggest that the 20% cold worked condition exhibits slightly better stress rupture behavior than the 10% condition.

Results: Creep Rupture

The thermal creep studies shown in Figures 2 and 3 indicate that increasing the cold work level at 550°C causes thermal creep to decrease at all stress levels investigated. The same behavior is observed at low stress levels at 605°C, but the role of cold work reverses between 109 and 152 MPa at 605°C, and higher levels of creep occur with increasing cold work. At temperatures above 605°C increasing levels of cold work always increased thermal creep.

The in-reactor experiments were conducted not only at temperatures comparable to those of the thermal studies but also at lower temperatures, where thermal creep is negligible but irradiation creep and swelling are important. As shown in Figure 4, the effect of cold work level on the total strain at 400°C is second order in importance compared to the influence of stress level. There is, however, a reversal in the influence of cold work level on the total strain between 60 and 100 MPa. This reversal is also evident in the stress-normalized creep curves that are shown in Figures 5a-5c. Figure 5d demonstrates that cold work at 400°C is also expressed in its influence on the upper and lower boundaries of the normalized creep curves, first expanding the range of normalized creep strain with stress level at the 20% cold work level, and then raising both the upper and lower limits of the response at the 30% level. The non-monotonic variability in the normalized strains at a given cold work level for such relatively low irradiation temperatures represents primarily the influence of stress in accelerating the development of void swelling.

Diametral strains are shown in Figures 6-8 for irradiation temperatures above 400°C. The rate of irradiation-induced diametral straining generally increases with cold work level at 495, 550 and 600°C, although reversals in behavior are often observed in both swelling and creep at relatively low stress levels. The impact of 30% cold work in significantly accelerating the creep rate becomes particularly obvious at 600°C. A similar reversal and acceleration were observed at 605°C in the thermal creep experiment (Figure 2). At 667°C, however, such reversals in behavior were not observed, and increasing cold work levels always accelerated creep, as shown in Figure 9. Figures 10-13 show the influence of cold work level on the normalized creep strains for irradiation temperatures above 400°C. Note that the impact of cold work differences becomes more pronounced with increased irradiation temperature. In particular, the tendency toward separation of the response band of different cold work levels increases with irradiation temperature, as demonstrated most strongly in Figure 13.

Results: Hardness Measurements

As shown in Figure 14, 30% cold work always leads to an eventual decline in hardness during aging relative to the hardness of the 10 and 20% cold work levels. The abruptness of this decline increases with increasing aging temperature. A similar but less pronounced trend is observed when comparing the 20% and 10% cold work levels. The drop in hardness is a direct measure of the degree of recovery experienced by the steel. A similar result has recently been published by Venkadesan and coworkers on an Indian version of this same steel.(7) Using smaller increments in cold work level than were employed in this study, they concluded that while the initial strength of the steel increased with cold work, levels greater than 17.5% led to a decline of the steel's properties during high temperature exposure. A similar conclusion was reached by Paxton for AISI 316 stainless steel.(8)

Discussion

The progressive influence of increasing cold work level on energy stored in a deformed material can be measured in terms of non-uniform lattice strain, as shown by Challenger and Lauritzen when they investigated the influence of cold work level on irradiation-induced swelling.[9] The lattice strain increases strongly from 0% to 20% cold work, as shown in Figure 15, but increases only an additional ~25% in the 20% to 30% cold work range, and very little more thereafter. With aging, the non-uniform lattice strain decreases somewhat; the largest and strongest changes occur at higher cold work levels, as demonstrated in Figure 15.

One would expect that the release of stored energy would be facilitated by the application of stress and that some temperature-dependent threshold stress would exist above which an accelerated release of stored energy would occur. This would be manifested as reversals in creep behavior with increasing stress level and was indeed observed in the high temperature irradiation and thermal creep studies presented in this paper. Similar observations in various steels have been made by other researchers, but the optimum cold work level depends on both the composition and irradiation environment.[5,10,11] In AISI 304, for example, the optimum cold work level was found to be only 10%.[10] This lightly alloyed steel is relatively weak compared to AISI 316 and other common stainless steels and does not offer as much resistance to recovery processes. The reversals with stress and the associated optimum cold work levels of other modified 316 steels have been found to vary with service temperature,[11] a finding consistent with the conclusions of this study.

The observed reversals during irradiation arise not only from thermally assisted processes, but also from other competing mechanisms. The release of stored energy and its associated effect on recovery provides the opportunity for some phases, particularly intermetallics, to form on moving grain fronts.[12,13] These phases often involve dimensional changes that contribute to the apparent creep strains.[14] It is known, however, that these phases are not only stress-sensitive in their rate of formation[15,16] but also subject to changes in composition arising from radiation-induced segregation.[17]

Another mechanism probably contributing to reversals in creep response arises from the conflicting roles of cold work in delaying void formation in stress-free materials[9,18,19] and the role of stress in promoting recovery of heavily cold worked material, a development which should promote void swelling. The onset of swelling is also known to be accelerated by stress even in the absence of cold work.[20-22] Additional complications involve the relationship between swelling and irradiation creep. Irradiation creep is also known to be proportional to the rate of swelling. Thus stress-enhanced swelling leads to an acceleration of creep.[23-25] Even before the onset of void swelling, the short-term transient regime of creep is known to be dependent on the stress state and initial cold work level.[26] In the absence of recovery, the transient ceases when the dislocation density has relaxed to its equilibrium level.

Conclusions

Based on the complexity of the competition between the various stress-sensitive and temperature-dependent processes discussed in the preceding section, it is not surprising that both thermal and irradiation creep exhibit non-monotonic behavior with respect to stress, temperature and cold work level. It is safe to state based on these studies, however, that increasing the cold work level of titanium-modified 316 from the conventional 20% level to 30% would be detrimental to its performance, especially at irradiation temperatures above 550°C. The driving force for the degradation of performance at the higher cold work level arises from the large level of non-uniform lattice strain induced during cold working and its release at high temperatures and stress levels.

The higher strength of 20% cold worked steel compared to that at 10% is not significantly offset by the differences in creep response. If it can be assumed that the response of this steel is typical of the alloy class, the 20% cold work level appears to be the optimum choice for the titanium-modified austenitic stainless steels employed in the U.S. fusion and breeder reactor materials programs.

References

1. H. R. Brager and F. A. Garner, in Effects of Radiation on Structural Materials, ASTM STP 683, J.A. Sprague and D. Kramer, Eds., American Society for Testing and Materials, 1979, pp. 207-232.

2. F. A. Garner, Journal of Nuclear Materials, 122-123 (1984) 459-471.

3. E. R. Gilbert and B. A. Chin, in Effects of Radiation on Materials: Tenth Conference, ASTM STP 725, D. Kramer, H. R. Brager and J. S. Perrin, Eds. American Society for Testing and Materials, 1981, pp. 665-679.

4. R. J. Puigh and R. E. Schenter, in Effects of Radiation on Materials: Twelfth International Symposium, ASTM STP 870, F. A. Garner and J. S. Perrin, Eds., American Society for Testing and Materials, 1985, pp. 795-802.

5. R. A. Moen and D. R. Duncan, Hanford Engineering Development Laboratory Report, HEDL-TI-76005, March 1976.

6. R. J. Puigh and M. L. Hamilton, in Influence of Radiation on Materials Properties: Thirteenth International Symposium (Part II), ASTM STP 956, F. A. Garner, C. H. Henager, Jr., and N. Igata, Eds., American Society for Testing and Materials, 1987, pp. 22-29.

7. S. Venkadesan, A. K. Bhaduri and P. Rodriguez, pp. 249-254 in Fast Reactor Core and Fuel Structural Behavior, BNES, London, June 1990, pp. 249-254.

8. M. M. Paxton, Hanford Engineering Development Laboratory Report, HEDL-TME-74-11, February 1974.

9. K. D. Challenger and T. Lauritzen, in Properties of Reactor Structural Materials After Neutron or Particle Irradiation, ASTM STP 570, C. J. Barodi and F. R. Shobers, Eds., 1975, pp. 388-403.

10. L. Bernard, E. Campo and S. Quarantra, in Mechanical Behavior and Nuclear Applications of Stainless Steel at Elevated Temperatures, The Metals Society, London, May 1981, pp. 88-93.

11. Y. Kondo, T. Yukitoshi, K. Yoshikawa, N. Nagai, S. Ohta, M. Fujiwara, S. Yoshida, C. Tanaka, K. Uematsu and K. Suzuki, in Radiation Effects in Breeder Reactor Structural Materials, M. L. Bleiberg and J. W. Bennett, Eds., The Metallurgical Society, New York, June 1977, pp. 253-267.

12. B. Weiss and R. Stickler, Metallurgical Transactions, 3 (1972), pp. 851-866.

13. F. A. Garner, F. Abe and T. Noda, Journal of Nuclear Materials, 155-157 (1988), pp. 870-876.

14. R. J. Puigh, A. J. Lovell and F. A. Garner, Journal of Nuclear Materials, 122 & 123 (1984) 242-245.

15. F. A. Garner, in Damage Analysis and Fundamental Studies Quarterly Progress Report, DOE/ER-0046/5, May 1981, pp. 198-218.

16. K. C. Russell and F. A. Garner, in Damage Analysis and Fundamental Studies Quarterly Progress Report, DOE/ER-0046/7, November 1981, pp. 180-197.

17. W. J. S. Yang, in Radiation-Induced Changes in Microstructure, ASTM STP 955, F. A. Garner, N.H. Packan and A. S. Kumar, Eds., American Society for Testing and Materials, 1987, pp. 628-646.

18. H. R. Brager and F. A. Garner, in Effects of Radiation on Structural Materials, ASTM STP 683, J. A. Sprague and D. Kramer, Eds., American Society for Testing and Materials, 1979, pp. 207-232.

19. H. R. Brager, Journal of Nuclear Materials, 57, (1975), 103.

20. F. A. Garner, E. R. Gilbert and D. L. Porter, in Ref. 3, pp. 680-697.

21. T. Lauritzen, S. Vaidyanathan, W. L. Bell and W. J. S. Yang, in Radiation-Induced Changes in Microstructure, 13th International Symposium (Part I), ASTM STP 955, F. A. Garner, N. H. Packan and A. S. Kumar, Eds., American Society for Testing and Materials, 1987, pp. 101-103.

22. D. L. Porter, M. L. Takata and E. L. Wood, Journal of Nuclear Materials, 116, (1983), pp. 272-276.

23. F. A. Garner and R. J. Puigh, Journal of Nuclear Materials, 179-181 (1991), pp. 577-580.

24. D. L. Porter, G. D. Hudman and F. A. Garner, Journal of Nuclear Materials, 179-181 (1991), pp. 581-584.

25. F. A. Garner and D. L. Porter, Journal of Nuclear Materials, 155-157 (1988), pp. 1006-1011.

26. M. B. Toloczko, F. A. Garner and C. R. Eiholzer, "Determination of Creep-Swelling Coupling Coefficients for Irradiated Stainless Steels", Fusion Reaction Materials Semiannual Progress Report, DOE/ER-0313/9, 1991.

27. E. R. Gilbert and B. A. Chin, Nuclear Technology, 52 (1981) 273-283.

Figure Captions

1. Comparison of the thermal and in-reactor stress rupture behavior of 10% and 20% cold worked D9.
2. Thermal creep observed at 550 and 605°C for various cold work levels.
3. Thermal creep observed at 670 and 760°C for various cold work levels.
4. Deformation induced by irradiation creep and swelling at 400°C for three cold work levels. Open and closed data points are identical and are used only to differentiate closely spaced data.
5. Normalized creep strains for pressurized tubes irradiated at 400°C. This treatment assumes that swelling is not affected by stress.
6. Diametral strains observed in tubes irradiated at 495°C.
7. Diametral strains observed in tubes irradiated at 550°C.
8. Diametral strains observed in tubes irradiated at 600°C.
9. Diametral strains observed in tubes irradiated at 667°C.
10. Normalized creep strains for pressurized tubes irradiated at 495°C.
11. Normalized creep strains for pressurized tubes irradiated at 550°C.
12. Normalized creep strains for pressurized tubes irradiated at 600°C.

13. Normalized creep strains for pressurized tubes irradiated at 667°C.

14. Hardness following thermal aging as a function of initial cold work level.

15. Root mean strain as a function of cold work level and thermal aging for AISI 316, as measured by Challenger and Lauritzen using x-ray line broadening.[9]

①

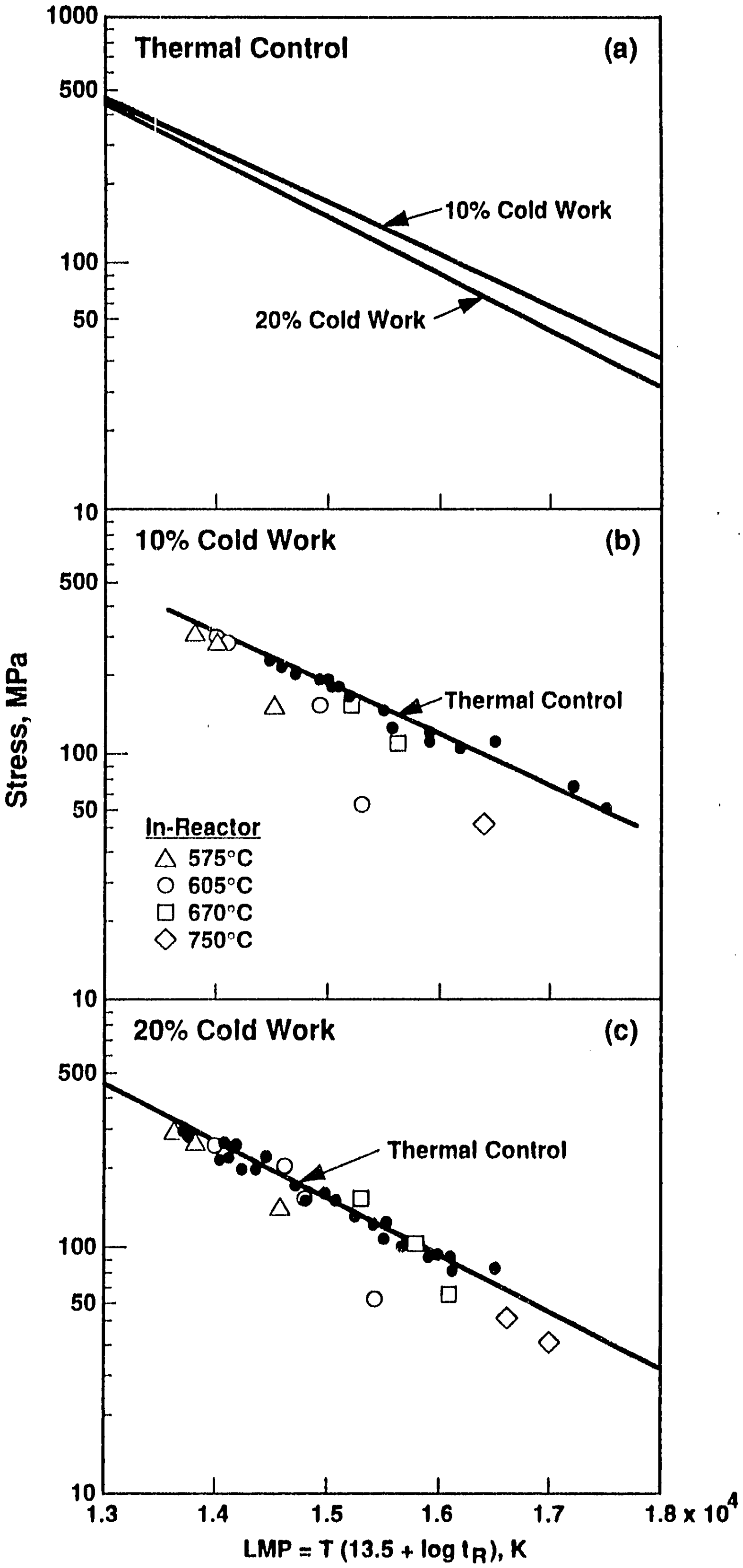

39107088.10

2

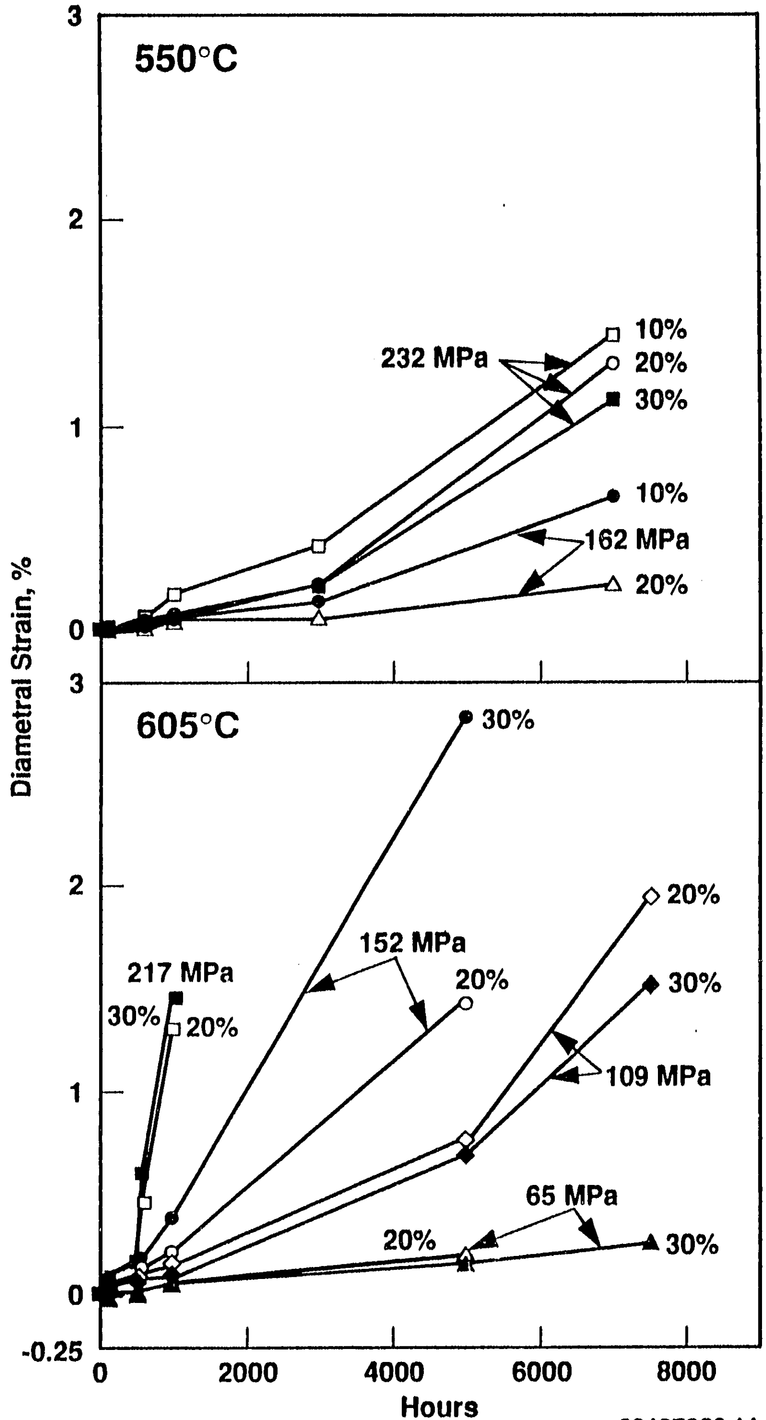

39107088.11

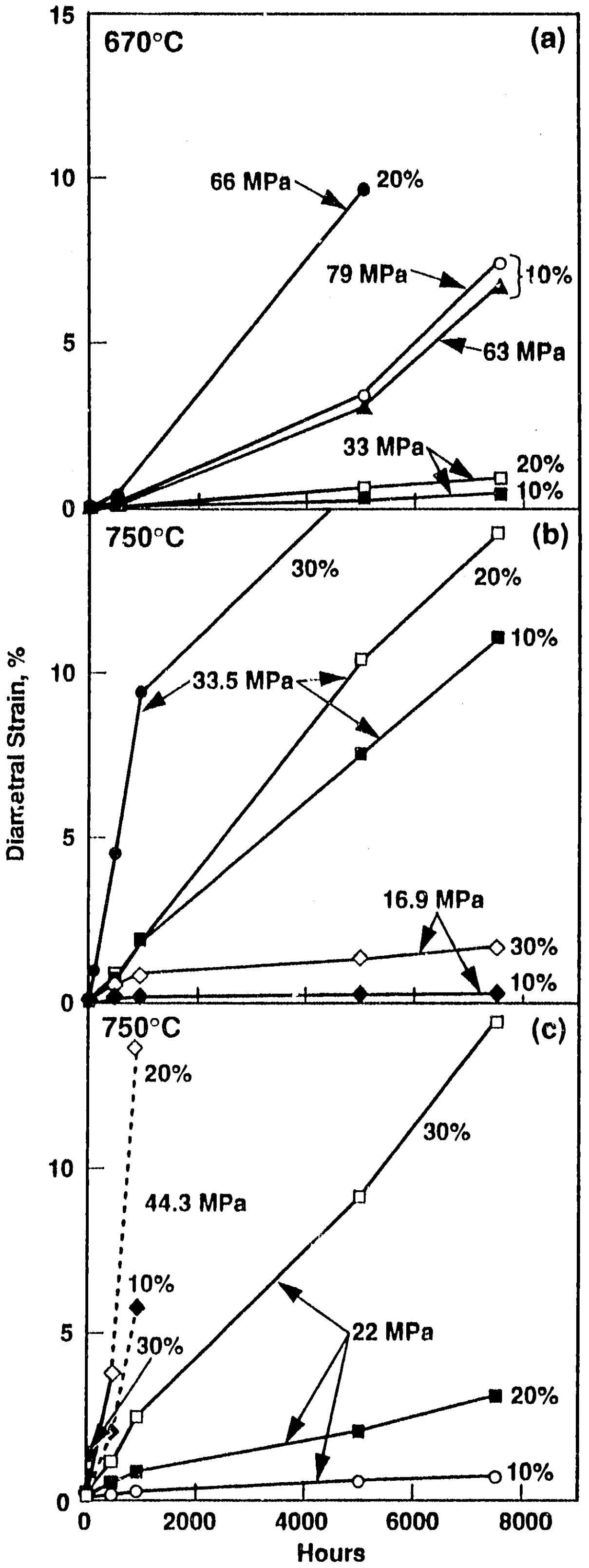
670°C
(a)
66 MPa
20%
79 MPa
10%
63 MPa
33 MPa
20%
10%
750°C
(b)
30%
20%
10%
33.5 MPa
16.9 MPa
30%
10%
750°C
(c)
20%
30%
44.3 MPa
10%
22 MPa
30%
20%
10%
Diametral Strain, %
Hours
0
5
10
15
2000
4000
6000
8000

39107088.12

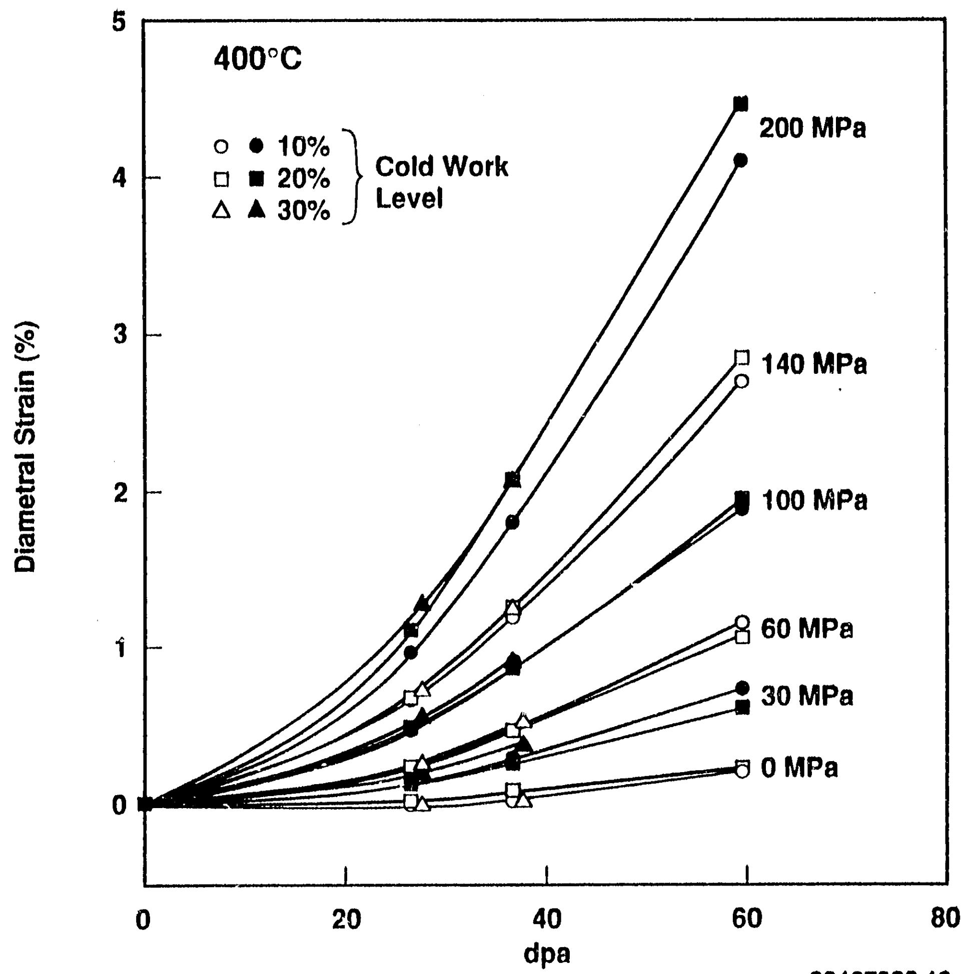

39107088.13

OK

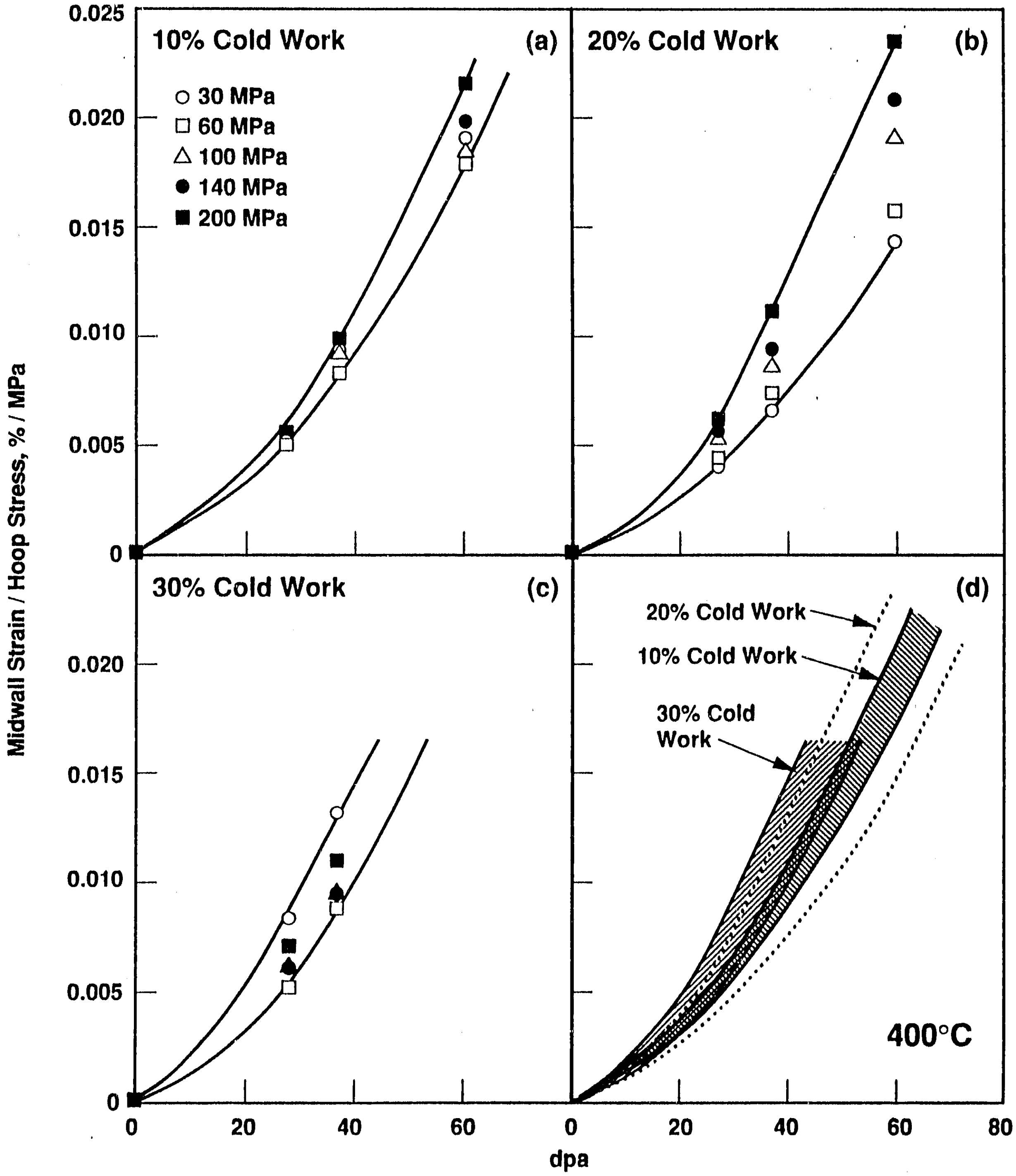
10% Cold Work
(a)
30 MPa
60 MPa
100 MPa
140 MPa
200 MPa
20% Cold Work
(b)
30% Cold Work
(c)
(d)
20% Cold Work
10% Cold Work
30% Cold Work
400°C
Midwall Strain / Hoop Stress, % / MPa
0.025
0.020
0.015
0.010
0.005
0
0
20
40
60
80
dpa

39107088.14

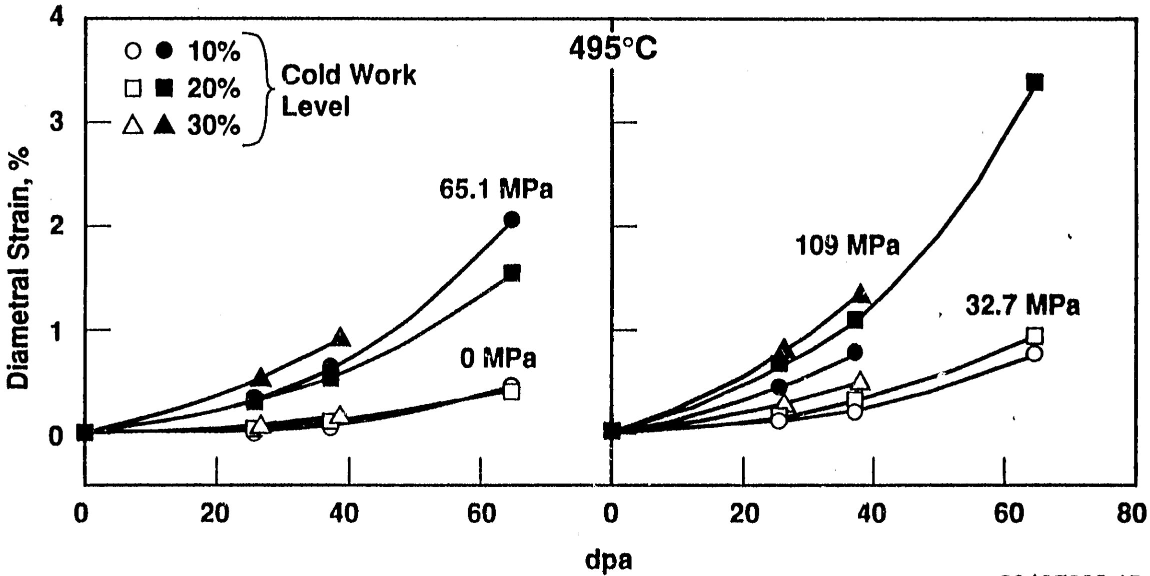

4
3
2
1
0
Diametral Strain, %
10%
20%
30%
Cold Work Level
495°C
65.1 MPa
0 MPa
109 MPa
32.7 MPa
0
20
40
60
0
20
40
60
80
dpa

39107088.15

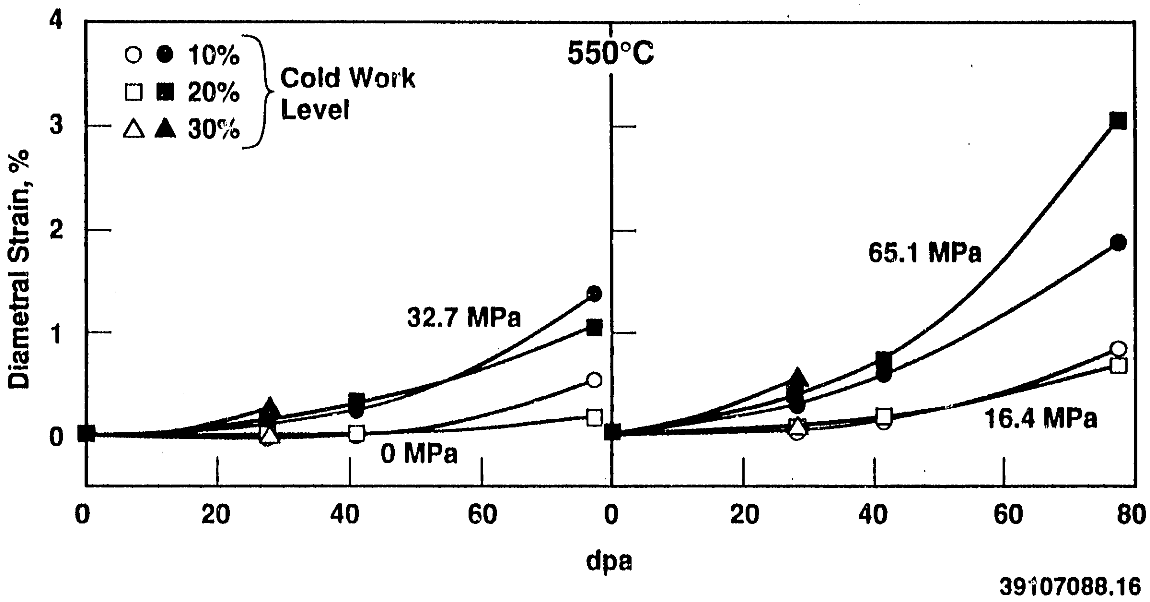
4
3
2
1
0
Diametral Strain, %
10%
20%
30%
Cold Work Level
550°C
32.7 MPa
0 MPa
65.1 MPa
16.4 MPa
0
20
40
60
0
20
40
60
80
dpa
39107088.16

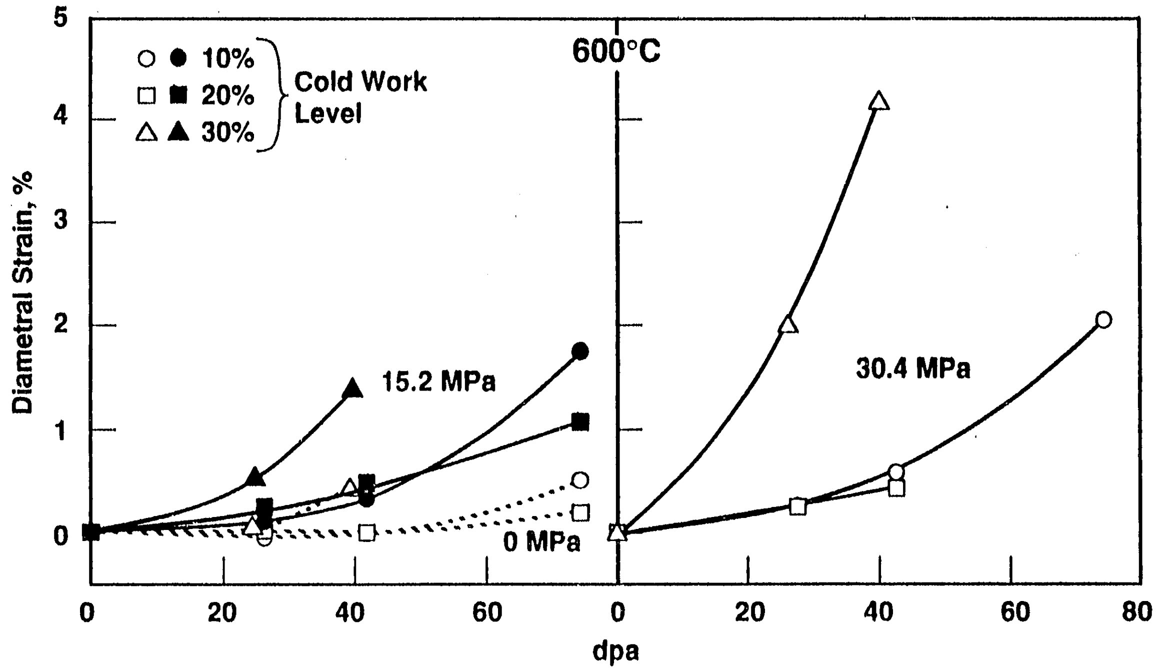
600°C
○ ● 10%
□ ■ 20%
△ ▲ 30%
Cold Work Level
Diametral Strain, %
15.2 MPa
0 MPa
30.4 MPa
dpa
0
1
2
3
4
5
0
20
40
60
80

39107088.17

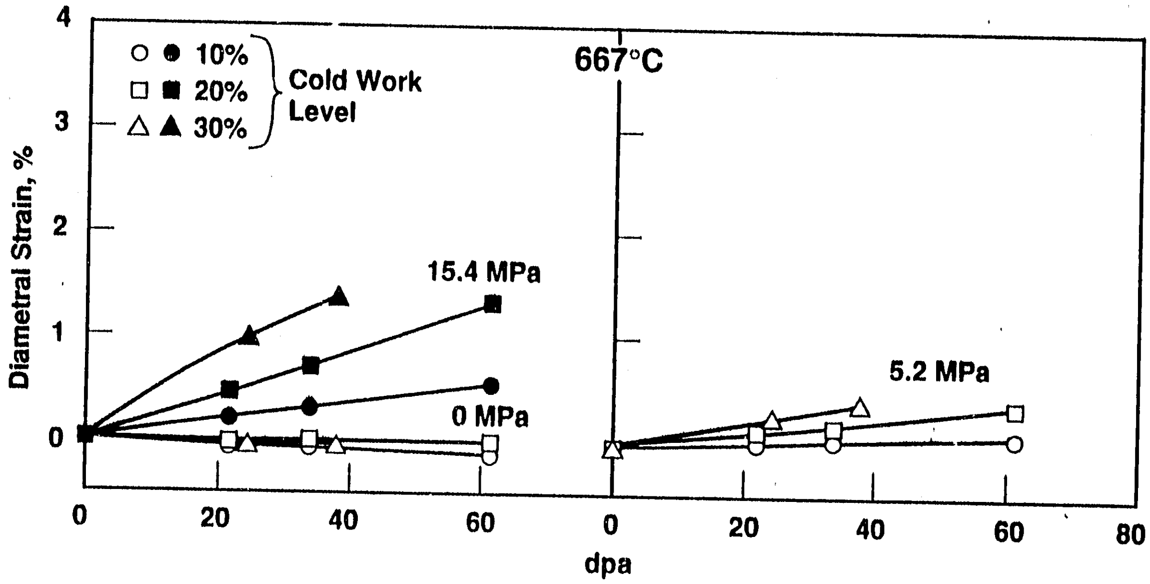

4
3
2
1
0
○ ● 10%
□ ■ 20%
△ ▲ 30%
Cold Work
Level
667°C
Diametral Strain, %
15.4 MPa
0 MPa
5.2 MPa
0
20
40
60
0
20
40
60
80
dpa

39107088.18

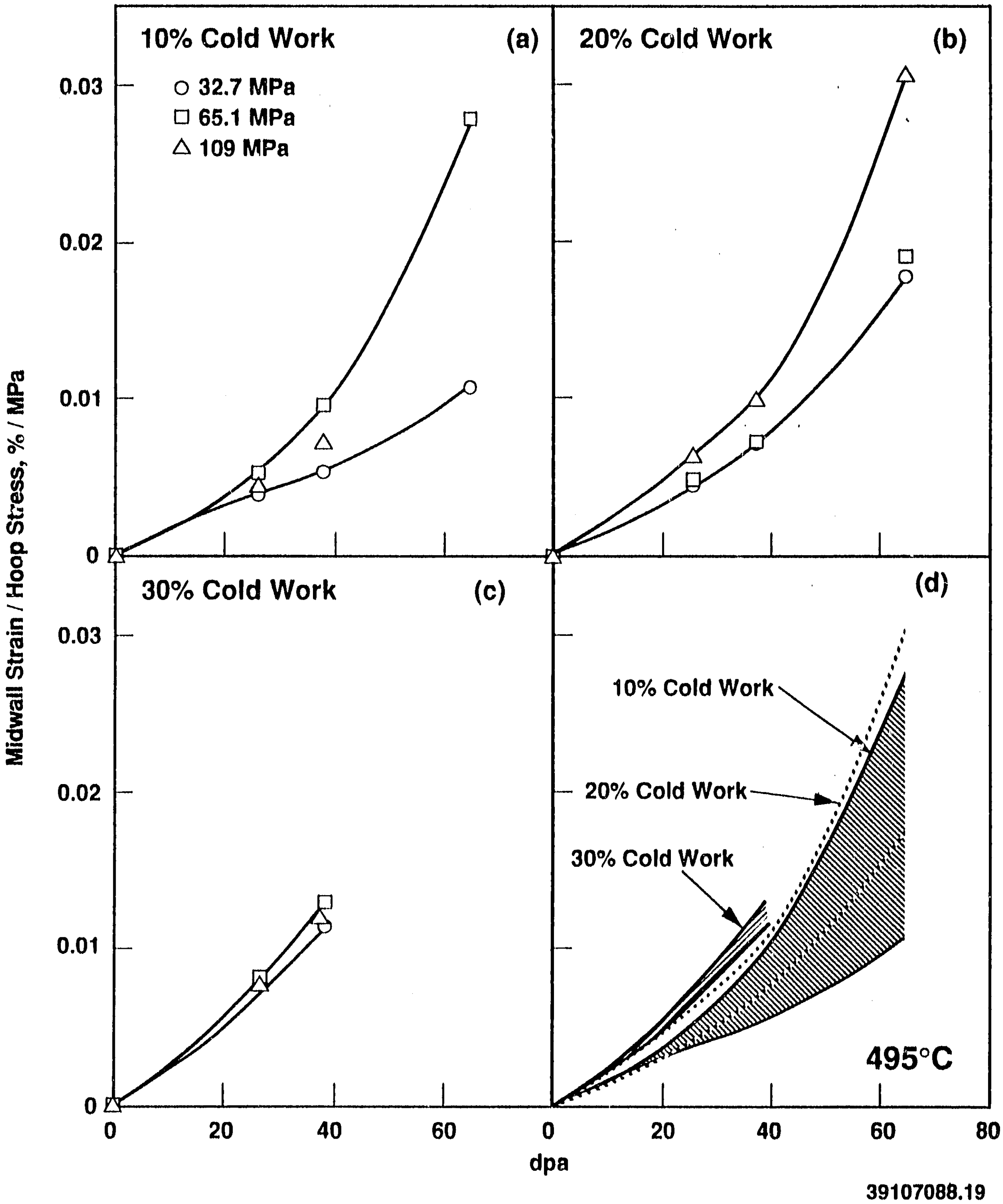
10% Cold Work
(a)
○ 32.7 MPa
□ 65.1 MPa
△ 109 MPa
20% Cold Work
(b)
30% Cold Work
(c)
(d)
10% Cold Work
20% Cold Work
30% Cold Work
495°C
Midwall Strain / Hoop Stress, % / MPa
0
0.01
0.02
0.03
0
20
40
60
80
dpa
39107088.19

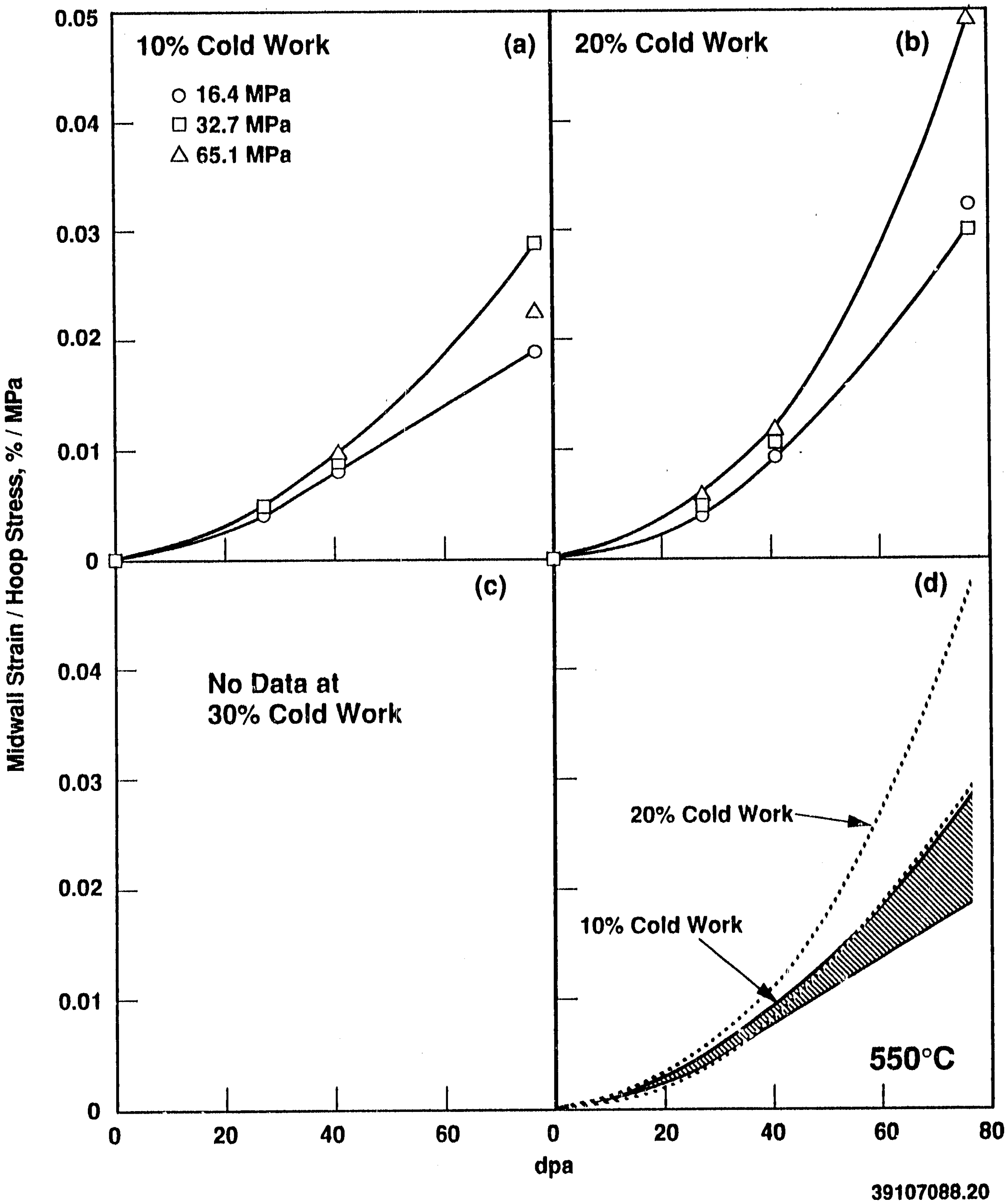
10% Cold Work
(a)
○ 16.4 MPa
□ 32.7 MPa
△ 65.1 MPa
20% Cold Work
(b)
(c)
No Data at
30% Cold Work
(d)
20% Cold Work
10% Cold Work
550°C
Midwall Strain / Hoop Stress, % / MPa
dpa
0.05
0.04
0.03
0.02
0.01
0
20
40
60
80
39107088.20

U

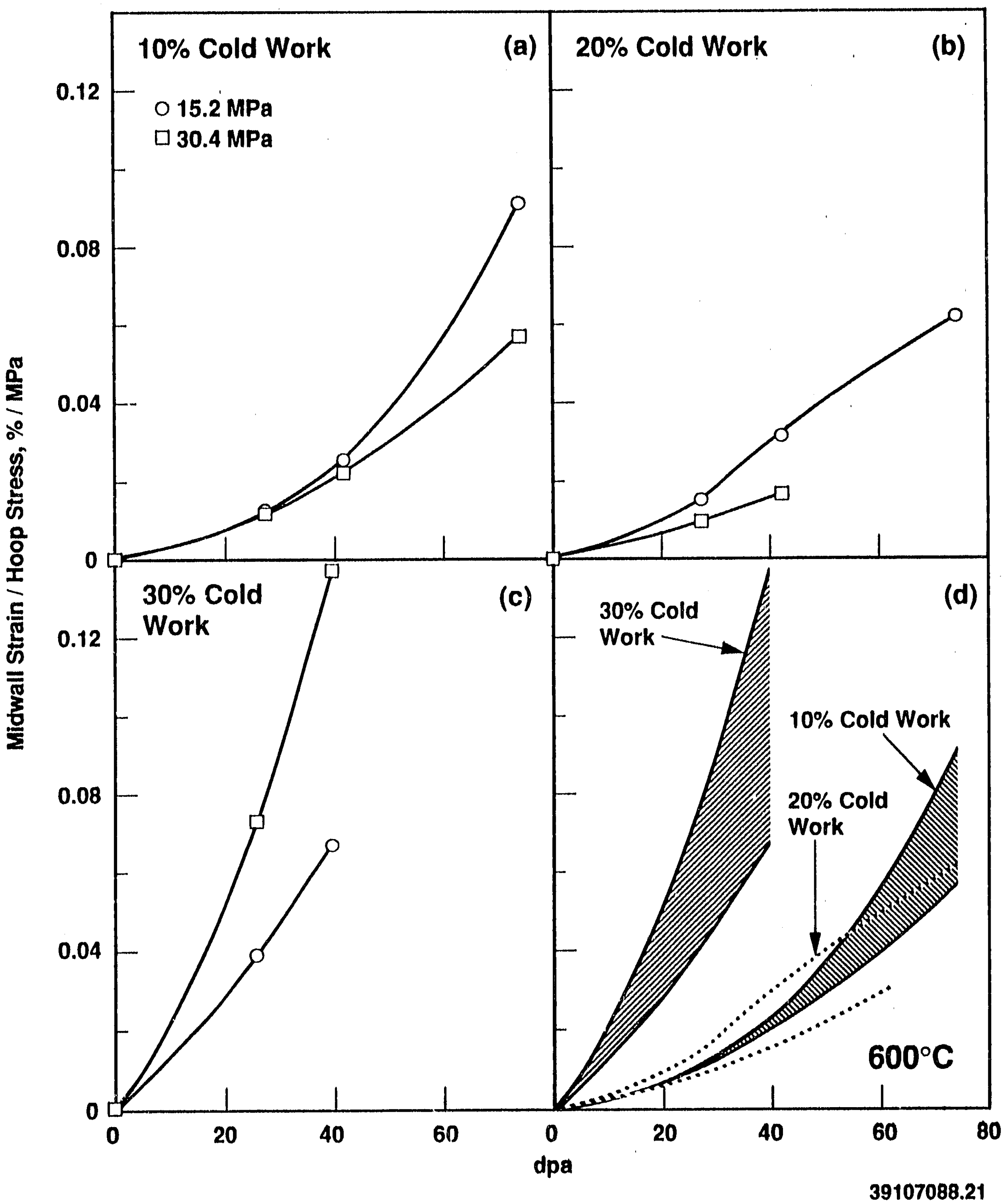

10% Cold Work
(a)
○ 15.2 MPa
□ 30.4 MPa
20% Cold Work
(b)
30% Cold Work
(c)
(d)
30% Cold Work
10% Cold Work
20% Cold Work
600°C
0.12
0.08
0.04
0
0
20
40
60
80
Midwall Strain / Hoop Stress, % / MPa
dpa
39107088.21

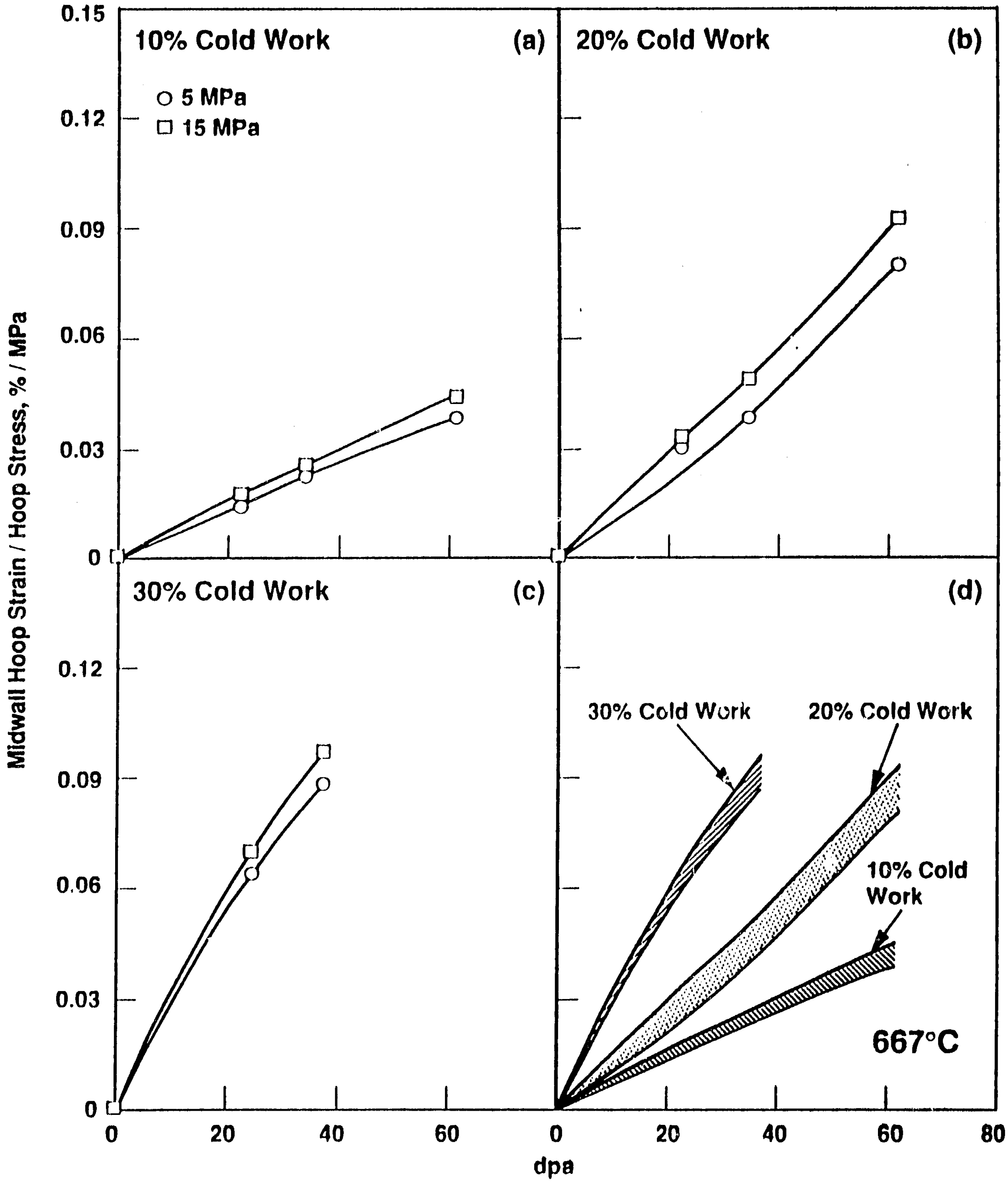

0.15
0.12
0.09
0.06
0.03
0
10% Cold Work
(a)
○ 5 MPa
□ 15 MPa
20% Cold Work
(b)
30% Cold Work
(c)
(d)
30% Cold Work
20% Cold Work
10% Cold Work
667°C
Midwall Hoop Strain / Hoop Stress, % / MPa
0
20
40
60
80
dpa

39107088.22

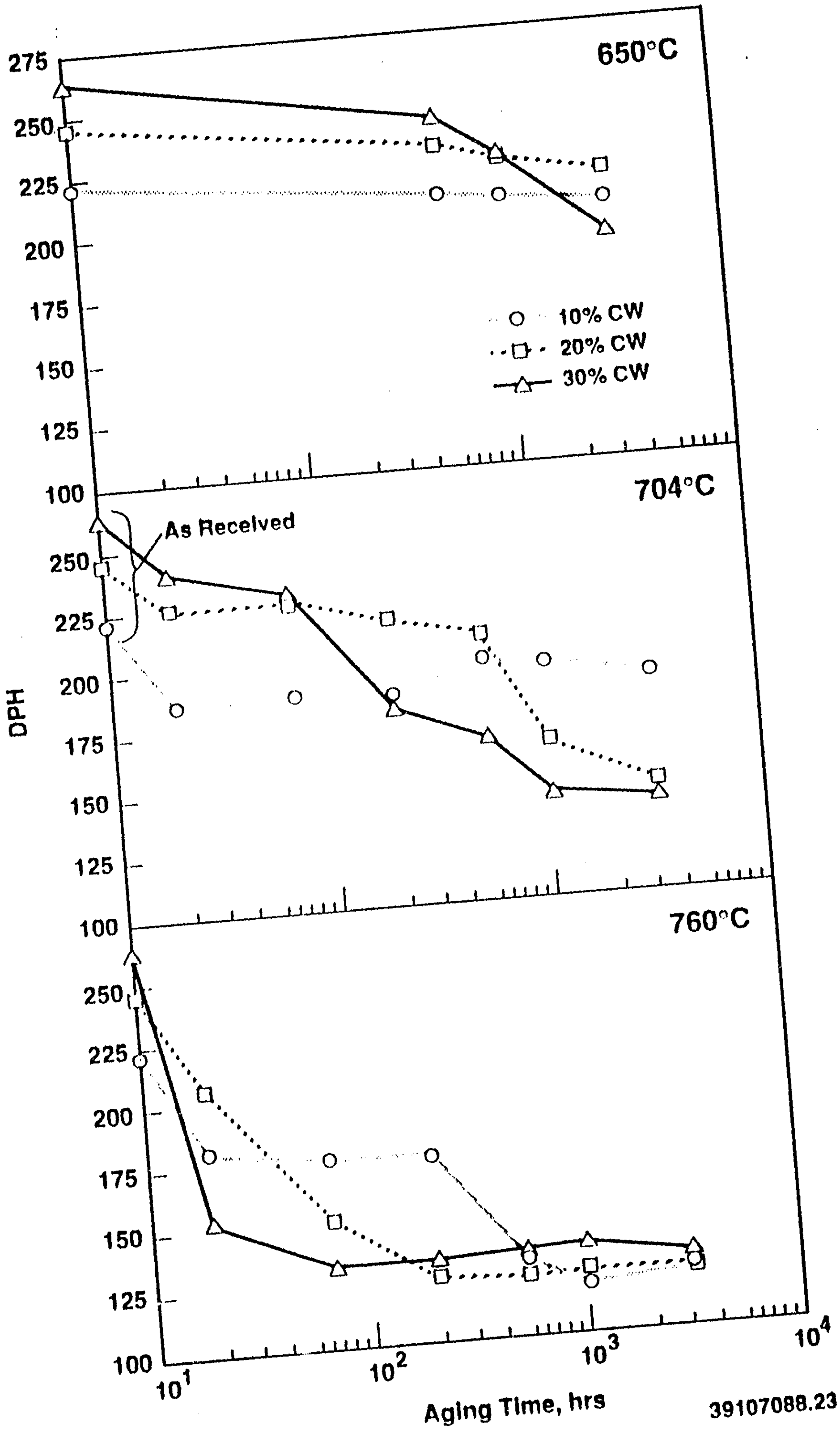
650°C
704°C
760°C
10% CW
20% CW
30% CW
As Received
DPH
275
250
225
200
175
150
125
100
10^1
10^2
10^3
10^4
Aging Time, hrs
39107088.23

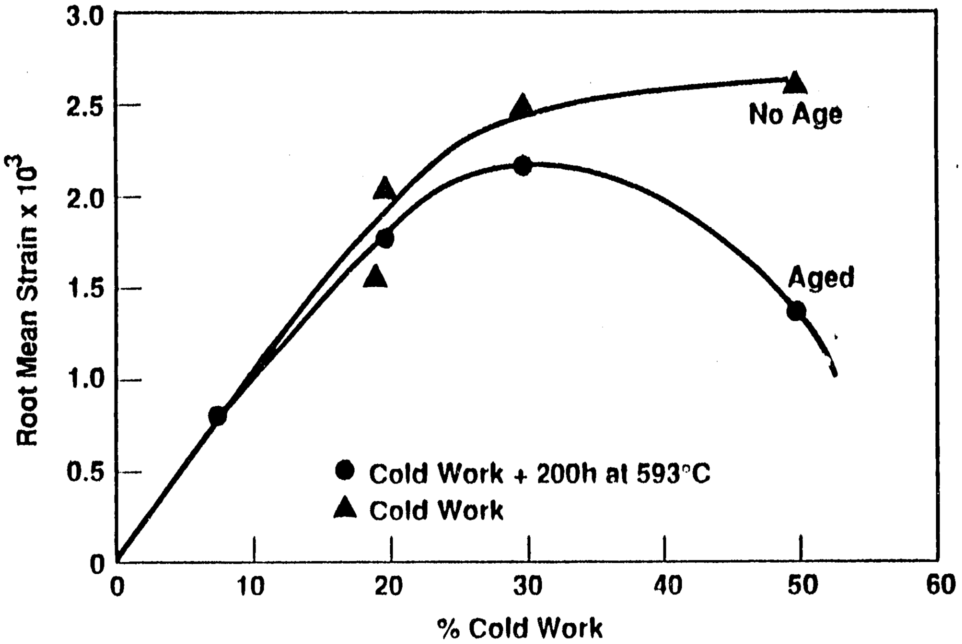
3.0
2.5
2.0
1.5
1.0
0.5
0
Root Mean Strain x 10^3
No Age
Aged
Cold Work + 200h at 593°C
Cold Work
0
10
20
30
40
50
60
% Cold Work

39107088.8

END

DATE FILMED

2/21/92

I